

# Supplementary Material

“CNN-PS: CNN-based Photometric Stereo for General Non-Convex Surfaces”

Satoshi Ikehata

**Abstract.** This supplementary appends some important discussions and data that were not included in the main paper due to the space limit. First, we discuss the issue of BEAR in *DiLiGenT* datasets as was described in Sec.5.4 (Appendix A). Second, we refer the 3-D models used to render images in the *CyclesPS* and *CyclesPSBench* datasets (Appendix B). Third we provide a complete visual comparison on the *CyclesPSBench* dataset (Appendix C). Forth, we provide complete quantitative and visual comparisons on the *DiLiGenT* dataset (Appendix D).

## 1 Appendix A: The problem in the BEAR dataset

As described at Table 2 in the main paper, we discarded first 20 images in BEAR dataset since some images in BEAR were found to be corrupted. This issue is illustrated in Fig. 1. We observed that the intensity values around the stomach region of the bear are lower than adjacent region in spite that they should be higher because of the specularities. We do not know the exact cause of the issue (the sensor saturation may not explain about this issue), but we observed this phenomenon only in the first 20 images in the BEAR dataset. We should note that the mean angular errors of some model-based algorithms slightly decreased when we discarded first 20 images of BEAR in the same manner with us (*i.e.*, from 6.1 to 5.2 degrees for ST14 and from 7.1 to 5.8 degrees for IA14), however ones of robust algorithms did not change dramatically (*i.e.*, from 4.79 to 4.78 for IW14 and 6.9 to 6.4 for IW12) simply because some problematic appearances had already been neglected as outliers.

## 2 Appendix B: The references to objects in *CyclesPS* and *CyclesPSBench* datasets

We rendered images in *CyclesPS* and *CyclesPSTest* datasets using the Cycles renderer with 3-D models collected from the internet. Fig. 2 illustrates complete references (*i.e.*, URLs) to those 3-D models. Both diffuse images and ground truth surface normal maps are also presented there.

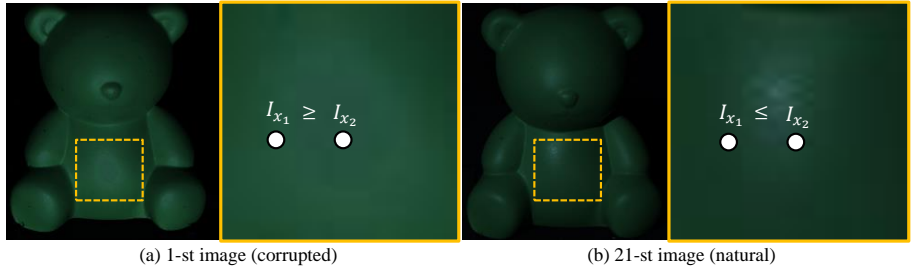


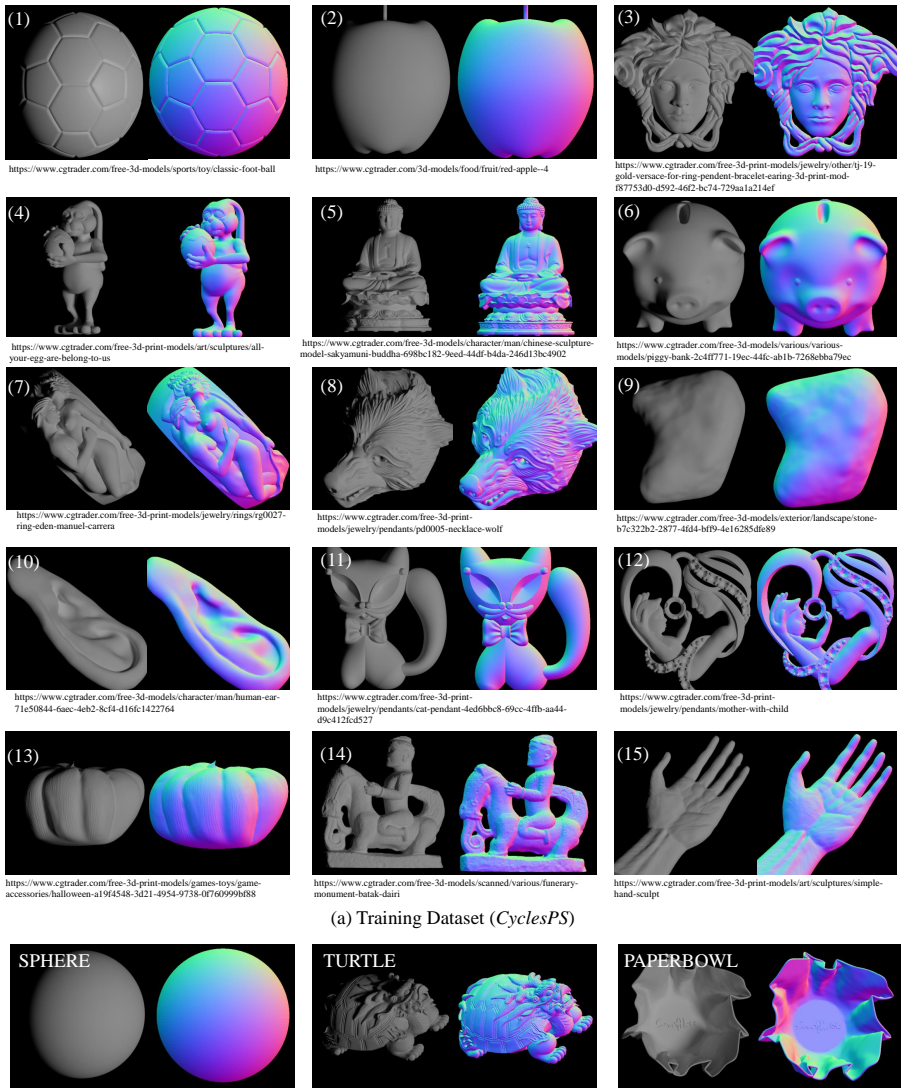
**Fig. 1.** The first 20 images in BEAR dataset has issues that intensity values around the stomach region ( $I_{x_2}$ ) are less than ones in the adjacent region ( $I_{x_1}$ ).

### 3 Appendix C: Full visual comparison on the *CyclesPSBench* dataset

Fig.3-6 illustrates the complete visual comparisons on the *CyclesPSBench* dataset that were not included in the main paper. Please see Table.1 and Fig.6 in the main manuscript for further details.

### 4 Appendix D: Full visual comparison on the *DiLiGenT* dataset

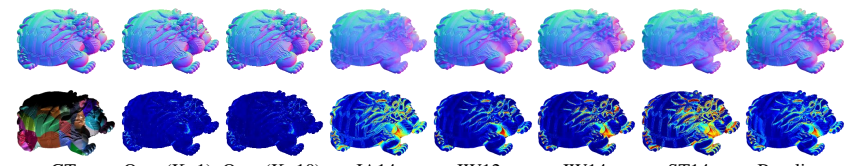
Table 1 illustrates the complete table of the quantitative comparison on the *DiLiGenT* dataset. We also show the complete visual comparisons in Fig.7-9. Please see further details in Sec.5.4 in the main paper. For each object, we compared our method (K=10) against TM18, IW14, ST14 and BASELINE. Note that the surface normal maps and error maps of TM18 were borrowed from their paper. We observed that our method worked better than other methods especially on the non-convex surfaces as we expected (e.g., inside the bag in the HARVEST, above the neck in BUDDHA and CAT).



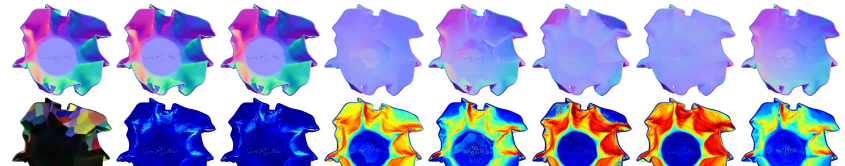
130 **Fig. 2.** The objects in *CyclesPS* and *CyclesPSBench* datasets.  
131  
132  
133  
134



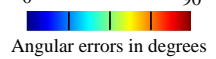
SPHERE (S), Uniform 305 lightings



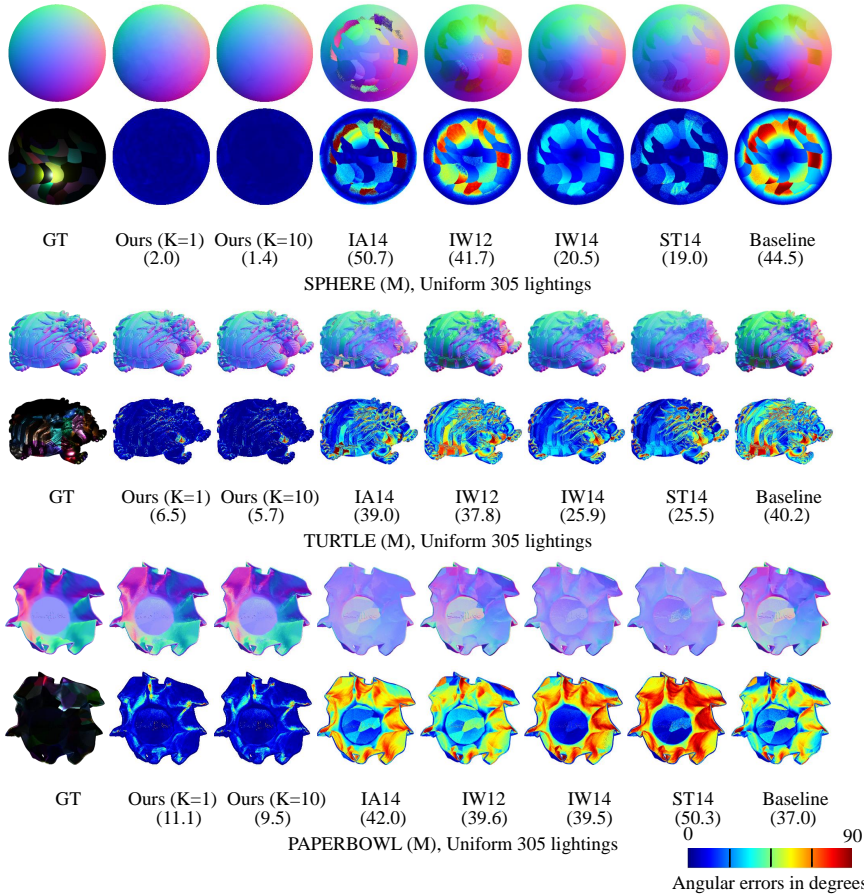
TURTLE (S), Uniform 305 lightings

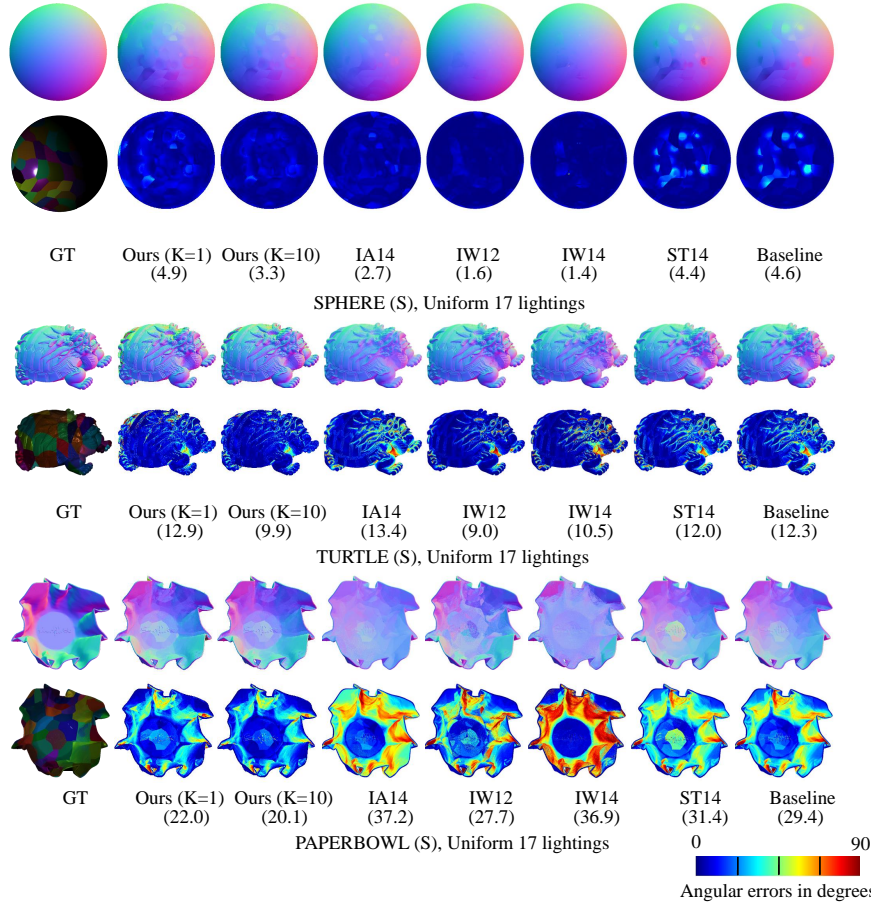


PAPERBOWL (S), Uniform 305 lightings



**Fig. 3.** Recovered surface normals and error maps for the *CyclesPSBench* dataset of Specular material. Images were rendered under uniform 305 lightings.





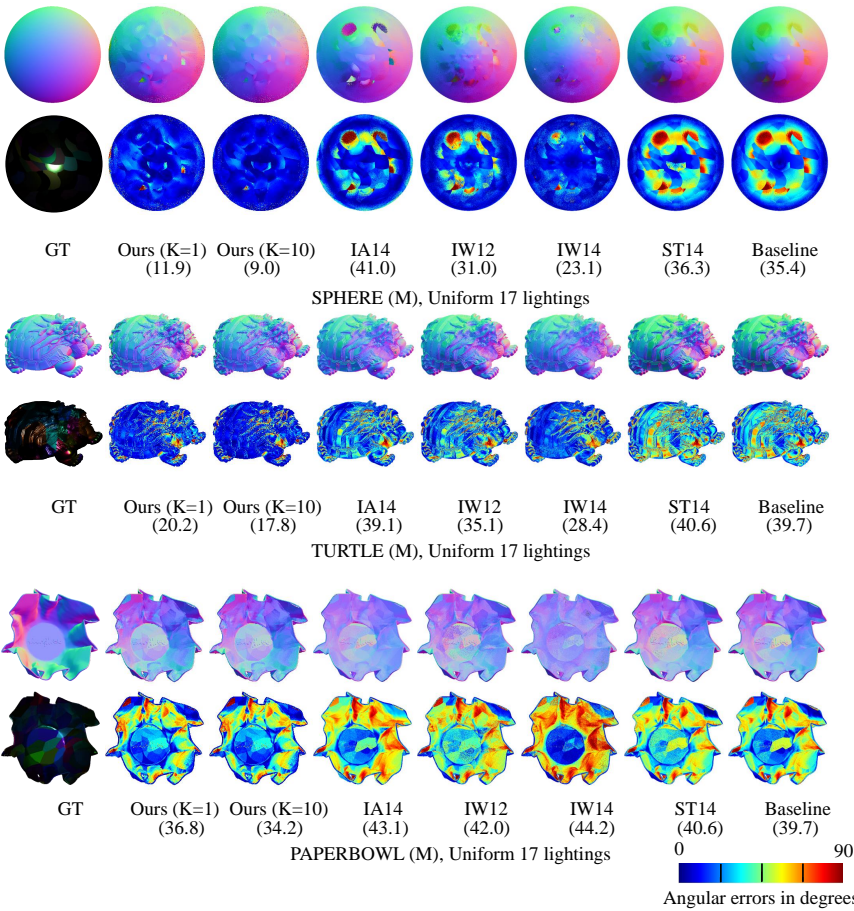


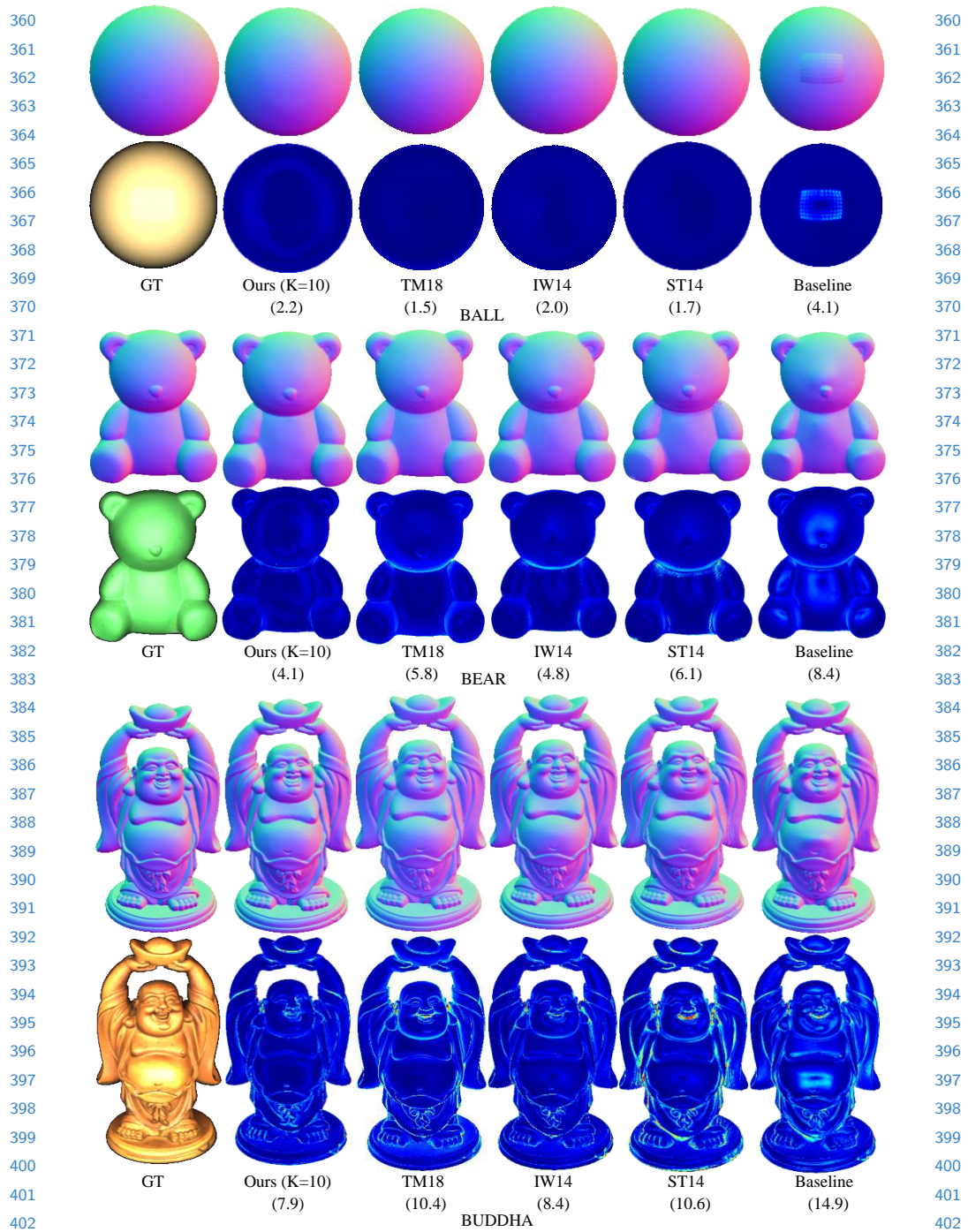
**Fig. 6.** Recovered surface normals and error maps for the *CyclesPSBench* dataset of Metallic material. Images were rendered under uniform 17 lightings.

315  
316  
317  
318  
319  
320  
321  
322  
323  
324  
325  
326  
327  
328  
329  
330  
331  
332  
333  
334  
335  
336  
337  
338  
339  
340  
341  
342  
343  
344  
345  
346  
347  
348  
349  
350  
351  
352  
353  
354  
355  
356  
357  
358  
359

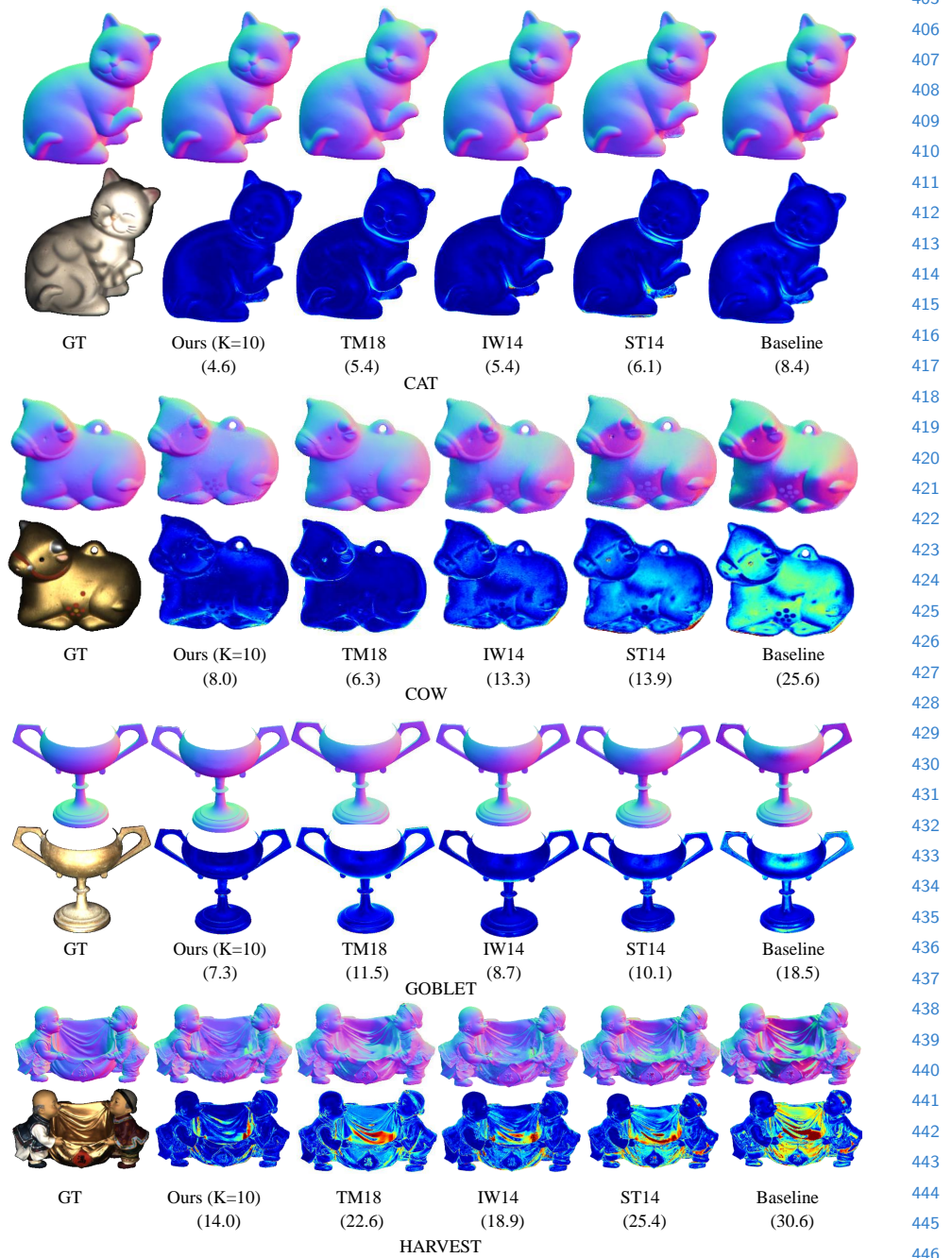
315  
316  
317  
318  
319  
320  
321  
322  
323  
324  
325  
326  
327  
328  
329  
330  
331  
332  
333  
334  
335  
336  
337  
338  
339  
340  
341  
342  
343  
344  
345  
346  
347  
348  
349  
350  
351  
352  
353  
354  
355  
356  
357  
358  
359

**Table 1.** Evaluation on the *DiLiGenT* dataset. We show the angular errors averaged within each object and over all the objects. (\*) Our method discarded first 20 images in BEAR since they are corrupted (See Appendix A).

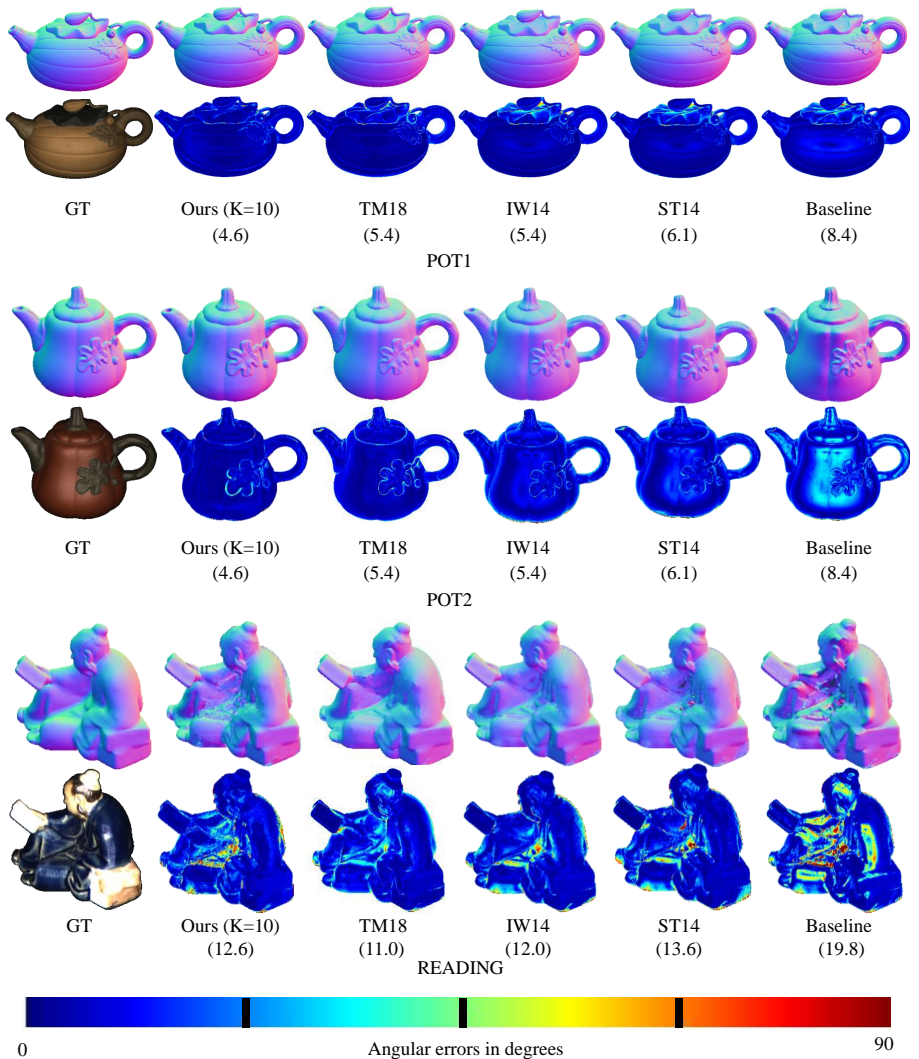
	BALL	BEAR	BUDDHA	CAT	COW	GOBLET	HARVEST	POT1	POT2	READING	AVE. ERR	RANK
OURS (K=10)	2.2	<b>4.1*</b>	<b>7.9</b>	<b>4.6</b>	8.0	7.3	<b>14.0</b>	5.4	<b>6.0</b>	12.6	<b>7.2</b>	1
OURS (K=1)	2.7	<b>4.5*</b>	8.6	5.0	8.2	<b>7.1</b>	14.2	5.9	6.3	13.0	<b>7.6</b>	2
HS17 [20]	<b>1.3</b>	5.6	8.5	4.9	8.2	<b>7.6</b>	<b>15.8</b>	<b>5.2</b>	6.4	12.1	<b>7.6</b>	2
TM18 [21]	1.5	5.8	10.4	5.4	<b>6.3</b>	11.5	22.6	6.1	7.8	<b>11.0</b>	8.8	4
IW14 [7]	2.0	4.8	8.4	5.4	13.3	8.7	18.9	6.9	10.2	12.0	9.0	5
SS17 [20]	2.0	6.3	12.7	6.5	8.0	11.3	16.9	7.1	7.9	15.5	9.4	6
ST14 [18]	1.7	6.1	10.6	6.1	13.9	10.1	<b>25.4</b>	6.5	8.8	13.6	10.3	7
SH17 [25]	2.2	5.3	9.3	5.6	<b>16.8</b>	10.5	24.6	7.3	8.4	13.0	10.3	7
IA14 [17]	3.3	7.1	10.5	6.7	13.1	9.7	<b>26.0</b>	6.6	8.8	14.2	10.6	9
GC10 [14]	3.2	6.6	14.9	8.2	9.6	14.2	27.8	8.5	7.9	<b>19.1</b>	12.0	10
AZ08 [13]	2.7	6.0	12.5	<b>6.5</b>	<b>21.5</b>	13.9	<b>30.5</b>	7.2	11.0	14.2	12.6	11
IW12 [6]	2.0	6.9	10.1	6.8	<b>27.6</b>	15.8	27.9	8.2	14.6	12.2	13.2	12
HM10 [15]	3.6	<b>11.5</b>	13.1	8.4	15.0	14.9	21.8	10.9	16.4	16.8	13.2	12
WG10 [5]	2.1	6.5	10.9	6.7	<b>25.9</b>	15.7	30.0	7.2	13.1	15.4	13.3	14
QW17[8]	2.3	6.6	13.8	7.7	<b>22.6</b>	16.2	<b>32.5</b>	8.6	11.6	16.1	13.8	15
ST12 [17]	13.6	19.4	18.4	12.3	<b>7.6</b>	17.8	19.3	10.4	9.8	17.2	14.6	16
BASELINE [12]	4.1	8.4	14.9	8.4	<b>25.6</b>	18.5	<b>30.6</b>	8.9	14.7	19.8	<b>15.4</b>	17



**Fig. 7.** Recovered surface normals and error maps for BALL, BEAR and BUDDHA in the *DiLiGenT* dataset.



**Fig. 8.** Recovered surface normals and error maps for CAT, COW, GOBLET and HARVEST in the *DiLiGenT* dataset.



488 **Fig. 9.** Recovered surface normals and error maps for POT1, POT2 and READING  
489 in the *DiLiGenT* dataset.  
490  
491  
492  
493  
494